# The First Epidermal Growth Factor-like Domain of the Low-Density Lipoprotein Receptor Contains a Noncanonical Calcium Binding Site†

Steven Malby,‡,§ Ruth Pickering,‡,§ Saurabh Saha,‡,§ Rachel Smallridge,‡ Sara Linse,|| and A. Kristina Downing*,‡

*Department of Biochemistry, Division of Structural Biology, University of Oxford, South Parks Road, Oxford OX1 3QU, U.K., Oxford Centre for Molecular Sciences, South Parks Road, Oxford OX1 3QT, U.K., and Department of Physical Chemistry 2, University of Lund, Chemistry Center, Lund, Sweden*

*Received October 4, 2000; Revised Manuscript Received November 22, 2000*

ABSTRACT: Removal of cholesterol-containing particles from the circulation is mediated by the low-density lipoprotein (LDL) receptor. Upon ligand binding, the receptor−ligand complex is endocytosed, and the ligand is released. The important biological role of the LDL receptor (LDLR) has been highlighted by the identification of more than 400 LDLR mutations that are associated with familial hypercholesterolemia. The extracellular region of the LDLR is modular in nature and principally comprises multiple copies of ligand binding, epidermal growth factor-like (EGF), and YWTD-type domains. This report describes characterization of the calcium binding properties of the tandem pair of EGF domains. While only the C-terminal EGF module contains the consensus sequence associated with calcium binding, a noncanonical calcium binding site in the N-terminal domain has been revealed using solution NMR spectroscopy. The calcium dissociation constants for the N- and C-terminal sites have been measured under physiologically relevant pH and ionic strength conditions using a combination of solution NMR, intrinsic protein fluorescence, and chromophoric chelator methods to be ∼50 $\mu$M and ∼10−20 $\mu$M, respectively. Identification of the novel calcium binding motif in LDLR sequences from other species suggests that it may confer specificity within the LDLR gene family. Comparison of the $K_d$ for the C-terminal site with the calcium concentration in late vesicles indicates that the binding properties of this module may be tuned to titrate upon endocytosis of the LDL receptor−ligand complex, and thus calcium binding may play a role in the ligand dissociation process.

The low-density lipoprotein receptor (LDLR)[1] is a transmembrane cell surface glycoprotein involved in removal of cholesterol esters from the circulation (reviewed in ref *1*). It binds to two types of lipoprotein, LDL and $\beta$-VLDL, via two ligand molecules, apolipoprotein B and apolipoprotein E. Upon ligand binding, the receptor is endocytosed and the ligand is discharged. It has been proposed that ligand dissociation is mediated by a pH-dependent change upon endocytosis from the extracellular space (∼7.4) to the endosomal compartment (∼5.0−5.5) (*2*). Dissociated lipoprotein is delivered to lysosomes where its cholesterol esters are hydrolyzed, and the LDLR is recycled to the cell surface.

More than 400 LDLR mutations have been identified which are associated with familial hypercholesterolemia (FH), a heritable disease of the cardiovascular system which predisposes to myocardial infarction (*3*). These mutations have been classified by Hobbs et al. (*4*) on the basis of their functional consequences, although the exact mechanisms by which disease is caused are not clear. While a genotype−phenotype relationship for FH has yet to be established, it appears that different regions of the protein may be associated with different pathogeneses.

The LDLR is a modular protein, and attempts have been made to dissect its functional properties on the basis of its domain organization (*5*, *6*). The extracellular ligand binding region comprises three types of domain, ligand binding (LDLR-A), epidermal growth factor-like (EGF), and YWTD (LDLR-B) (*7*, *8*) as shown in Figure 1A. Calcium is required for LDLR ligand binding (*9*), and structural data and amino acid sequence homology indicate that the LDLR-A domains as well as the second EGF domain contain calcium binding sites (*10*−*13*). Significant insight into the role of calcium in LDLR function has been provided by structural studies and measurements of the calcium binding properties of an

† This research was supported by the Wellcome Trust, the Biotechnology and Biochemistry Scientific Research Council, and the Medical Research Council. A.K.D. is a Wellcome Trust Senior Research Fellow. S.L. thanks the Swedish Natural Science Research Foundation and the Swedish Medical Research Foundation for support.

* To whom correspondence should be addressed. Tel/Fax: +44 (0)-1865 285322. E-mail: kristy@bioch.ox.ac.uk.

‡ University of Oxford and Oxford Centre for Molecular Sciences.

§ These authors contributed equally to this work.

|| University of Lund.

[1] Abbreviations: $\beta$-VLDL, $\beta$ very low density lipoprotein; cb, calcium binding; COSY, correlation spectroscopy; DNA, deoxyribonucleic acid; DTT, dithiothreitol; *E. coli*, *Escherichia coli*; EDTA, ethylenediaminetetraacetic acid; EGF, epidermal growth factor-like; LDL, low-density lipoprotein; EGF-A, first EGF domain of the LDLR; EGF-B, second EGF domain of the LDLR; FH, familial hypercholesterolemia; FPLC, fast-performance liquid chromatography; HPLC, high-pressure liquid chromatography; HSQC, heteronuclear single-quantum correlation; LDLR, low-density lipoprotein receptor; LDLR-A, low-density lipoprotein receptor ligand binding type; LDLR-B, low-density lipoprotein receptor YWTD type; NMR, nuclear magnetic resonance; NOESY, nuclear Overhauser enhancement spectroscopy; PCR, polymerase chain reaction; TFA, trifluoroacetic acid; TOCSY, total correlation spectroscopy.

10.1021/bi002322l CCC: $20.00 
Published on Web 01/27/2001

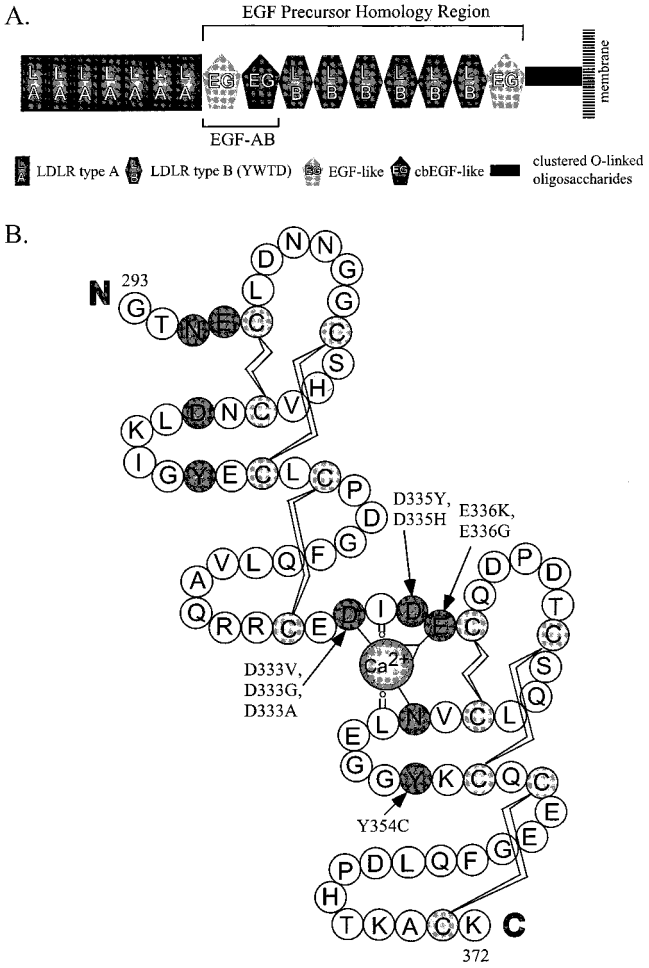


FIGURE 1: Domain organization of the extracellular region of the low-density lipoprotein receptor (A) and schematic illustration of the sequence and secondary structure of the EGF-AB pair (B). In (A) the positions of the EGF precursor homology region and the EGF-AB pair are indicated. In (B) partial and complete calcium binding consensus sequences are shaded in dark gray for the A and B domains, respectively. Cysteine residues which engage in disulfide bonds are shaded in light gray and are connected by jagged lines. Mutations which affect the calcium binding consensus sequence of the B domain are mapped onto the sequence. The calcium binding consensus sequence comprises a single aromatic residue which has been used previously to monitor calcium binding by cbEGF domains (*11*−*13*, *19*, *34*, *39*−*42*).

LDLR-A domain (*10*, *14*). The role of calcium binding to the EGF module(s) is not well understood, and a number of FH-associated mutations have been reported which are predicted to change residues in the calcium binding consensus sequence (*15*) (Figure 1B). In addition, studies of patients lacking the EGF precursor homology region (see Figure 1) or the EGF-AB pair suggest that these domains are involved in binding LDL and mediating acid-dependent dissociation of $\beta$-VLDL (*16*, *17*).

In this study we have characterized the calcium binding properties of the EGF-AB pair from the LDL receptor using solution nuclear magnetic resonance (NMR), intrinsic protein fluoresence, and chromophoric chelator methods. We have identified a noncanonical calcium binding site in the EGF-A domain which binds with higher affinity than any isolated or N-terminal calcium binding (cb) EGF domain which has been characterized to date. We have also determined the calcium dissociation constant for the EGF-B site localized between the two domains. We discuss the implications of these results for the functional properties of the intact LDL receptor.

## EXPERIMENTAL PROCEDURES

*Expression of the EGF-AB Domain Pair.* EGF domains A and B (corresponding to exons 7 and 8) of the LDLR were amplified by the polymerase chain reaction (PCR) from a human cDNA clone (kindly provided by Drs. Brian Knight and Anne Soutar). Forward and reverse primers were 5′-TAG TAG GGT ACC ATA GAA GGA CGA TCA GCA GGG ACC AAC GAA TGC TTG GAC AAC-3′ and 5′-TAG TAG AAG CTT CTA TTA CTT GCA GGC CTT CGT GTG GGG-3′, respectively. The primers were designed to amplify nucleotides corresponding to amino acids G293−K372 of the intact LDLR. In addition to the partial nucleotide sequences included in both primers, restriction sites (*Kpn*I in the forward primer and *Hin*dIII in the reverse) were included to facilitate cloning into the polylinker site of the pQE30 (Qiagen) vector which is downstream of a 6× histidine tag sequence. A factor Xa cleavage site was also included in the forward primer to enable removal of the His tag.

The DNA was initially used to transform *Escherichia coli* strain NM554 (*18*) containing a *lac* repressor plasmid (pREP4, Qiagen). Protein was produced and purified according to the methods described by Knott et al. (*19*). In brief, protein was harvested from inclusion bodies and applied to a column containing $Ni^{2+}$ or $Co^{2+}$ resin for initial purification. The column was washed, and the protein was eluted using a series of 6 M guanidine hydrochloride buffers with varying EDTA concentrations and/or pH. Protein was reduced using 0.1 M DTT in 0.1 M Tris·HCl, pH 8.3, and then directly refolded by dialysis against a solution containing 3 mM L-cysteine and 0.3 mM L-cystine in 50 mM Tris·HCl, pH 8.3, in the presence of 50 mM $Ca^{2+}$. The protein was reverse-phase HPLC purified using a C8 semipreparative column (Dynamax) and a gradient running from 20% to 80% of a buffer containing 80% acetonitrile/0.1% TFA over a time course of 40 min. The His tag was removed via cleavage with bovine factor Xa (Denzyme), at a ratio of 1:1000 enzyme to protein, in 50 mM Tris·HCl, pH 7.5, 0.1 M NaCl, and 1 mM $CaCl_2$ for 16 h. The protein was then subjected to two further rounds of chromatography, anion-exchange FPLC using a Mono-Q column (Pharmacia), and reverse-phase HPLC as described above. $^{15}N$ isotopically enriched samples were produced analogously using *E. coli* strains BL21[pREP4] and JM109, which were grown in minimal media with $^{15}NH_4Cl$ as the sole nitrogen source. Typical yields of purified protein were 2−5 mg/L of culture. Low-resolution electrospray mass spectrometry was used to confirm the molecular weight of the produced protein (data not shown).

*NMR Analysis of Protein Folding and Calcium Binding.* All NMR data were acquired using GE/home-built instruments. The properties of the LDLR EGF-AB construct were initially assayed using a sample containing ∼2 mM protein in 95% $H_2O$/5% $^2H_2O$ at pH 6.5. One-dimensional spectra were acquired with 2048 complex points and a spectral width of 8000 Hz at 500 MHz with solvent presaturation at temperatures of 25, 30, and 35 °C. All spectra showed

Table 1: NMR Data Acquisition Parameters

| sample | experiment | temp (°C) | spectral frequency (MHz) | complex points | | | acquisition time (ms) | | |
|---|---|---|---|---|---|---|---|---|---|
| | | | | $D_1$ | $D_2$ | $D_3$ | $F_3$ | $F_2$ | $F_1$ |
| (A) Proton-Specific Assignments, pH 6.5 | | | | | | | | | |
| EGF-AB, 95% $H_2O$/5% $^2H_2O$ | $^1H-^1H$ COSY, TOCSY, $t_m = 45$ ms | 25, 30 | 750 | 2048 | 350 | | | 164 | 28.0 |
| EGF-AB, 95% $H_2O$/5% $^2H_2O$ | $^1H-^1H$ NOESY, $t_m = 150$ ms | 25, 30 | 750 | 2048 | 400 | | | 164 | 32.0 |
| $^{15}N$ EGF-AB | $^1H-^{15}N$ HSQC | 30 | 600 | 1024 | 16 | | | 102 | 11.6 |
| $^{15}N$ EGF-AB | $^1H-^{15}N$ TOCSY-HSQC, $t_m = 40$ ms | 30 | 600 | 1024 | 16 | 64 | 102 | 11.6 | 6.4 |
| $^{15}N$ EGF-AB | $^1H-^{15}N$ NOESY-HSQC, $t_m = 150$ ms | 30 | 600 | 1024 | 16 | 150 | 102 | 11.6 | 15.0 |
| EGF-AB, 99.9% $^2H_2O$ | $^1H-^1H$ COSY, TOCSY, $t_m = 40$ ms | 25, 30 | 750 | 2048 | 375 | | | 164 | 30.0 |
| EGF-AB, 99.9% $^2H_2O$ | $^1H-^1H$ NOESY, $t_m = 150$ ms | 25, 30 | 750 | 2048 | 450 | | | 164 | 36.0 |
| (B) Calcium Titrations, pH 7.4 | | | | | | | | | |
| EGF-AB, 99.9% $^2H_2O$ | 1-D, HDO solvent presaturation | 30 | 600 | 4096 | | | | | 512.0 |
| $^{15}N$ EGF-AB | $^1H-^{15}N$ HSQC, ±2 mM EDTA | 30 | 600 | 1024 | 16 | | | 102 | 11.6 |
| EGF-AB, 95% $H_2O$/5% $^2H_2O$ | $^1H-^1H$ NOESY, $t_m = 150$ ms | 30 | 500 | 2048 | 256 | | | 256 | 32.0 |

narrow, Lorentzian line shapes, good HN chemical shift dispersion, and upfield-shifted methyl signals, characteristic of monomeric, folded protein. Optimal spectra were obtained at 30 °C, and this was selected as the temperature for further experiments. Spectra recorded at calcium concentrations of 0, 10, and 12 mM demonstrated calcium-dependent displacement of cross-peaks, which is associated with correct folding of cbEGF domains, and saturation of both sites at a calcium concentration of 10 mM (data not shown).

*Sequence-Specific Assignment of EGF-AB.* An additional NMR sample was prepared containing ~2.6 mM $^{15}N$-enriched EGF-AB, 5 mM Tris·HCl, 12 mM $CaCl_2$, and 0.02% $NaN_3$ in 95% $H_2O$/5% $^2H_2O$, pH 6.5, for the acquisition of $^{15}N$-edited data. The following spectra were acquired for the purpose of obtaining sequence-specific $^1H$ assignments: two-dimensional $^1H-^1H$ COSY (*20*, *21*), TOCSY (*22*, *23*), and NOESY (*24*, *25*), $^1H-^{15}N$ HSQC (*26*, *27*), and three-dimensional $^{15}N$-edited TOCSY-HSQC and NOESY-HSQC (*28*). In these experiments solvent suppression was normally achieved using pulsed-field gradients (*29*). Two-dimensional $^1H-^1H$ COSY, TOCSY, and NOESY spectra were also acquired after exchange of the unlabeled sample into 99.9% $^2H_2O$. Acquisition parameters for these experiments are given in Table 1. All spectra were processed using Felix 2.3 (MSI, Inc., San Diego, CA) typically using a 70° shifted squared sine-bell window function in the acquisition dimension and a Gaussian line-broadening window function, with −15 and 0.15 line broadening and Gaussian parameters, respectively, in the indirect dimension(s). A 0° shifted sine-bell window function was used in processing COSY spectra to resolve line splittings. Spectra were zero-filled as necessary to improve resolution, and linear prediction (*30*) was used to double the number of complex points in the $F_2$ ($^{15}N$) dimension of the HSQC and three-dimensional data sets. Sequence-specific $^1H$ and $^{15}N$ chemical shift assignments were made using conventional methods (*31*, *32*) with the program NMRView v.3.1.2 (*33*).

*NMR Measurement of EGF-A $K_d$.* An initial calcium titration was monitored by one-dimensional NMR using a 293 $\mu$M sample of EGF-AB dissolved in 99.9% $^2H_2O$, 5 mM Tris·HCl, and 150 mM NaCl, pH 7.4. This pH was chosen to more closely approximate physiological conditions. On the basis of the data from this titration, it became apparent that, upon calcium addition, the resonance corresponding to the H$\delta$* protons of the aromatic residue in the calcium binding site of EGF-B (which would normally be used to monitor calcium binding; see Figure 1B) sharpened but did not change position (Figure 2A). However, other peaks in the vicinity of the N-terminal region of the domain pair, e.g., the H$\gamma$2* resonance of Thr 294, shifted significantly (Figure 2B). These observations led to two conclusions: (i) that the EGF-B site was saturated with a paramagnetic contaminant (e.g., $Mn^{2+}$) following HPLC protein purification which could be competed out by $Ca^{2+}$ and (ii) that the EGF-A domain contains a noncanonical calcium binding site. Conclusion ii rested on the observations that residue Thr 294 is at the N-terminus of the construct, and far removed from the calcium binding site in domain B, and that the interdomain linker is not long enough to accommodate juxtaposition of the two sites (see Figure 1B). To test the first hypothesis, two-dimensional HSQC spectra were acquired in 95% $H_2O$/5% $^2H_2O$, 150 mM NaCl, and 5 mM Tris·HCl, pH 7.4, at 30 °C in the presence and absence of 2 mM EDTA, on samples containing ~300 and ~385 $\mu$M LDLR EGF-AB, respectively. Comparison of these data revealed a large change in the spectrum associated with the addition of EDTA, corresponding to removal of calcium from the EGF-B site (Figure 2C). To test the possibility that the peak broadening in Figure 2A might have arisen from intermediate time scale exchange, two-dimensional spectra were acquired, using the parameters for the calcium titration described below, in the presence of EDTA or saturating calcium. A comparison of these spectra demonstrated that removal of calcium from the B-site led to migration of the Tyr 354 H$\delta$*−H$\epsilon$* cross-peak as a single peak, which is not consistent with exchange (data not shown).

To measure calcium dissociation constants for the EGF-A site, a sample was prepared containing 1.125 mg of EGF-AB in 1 mL of 99.9% $^2H_2O$. The sample was passed through a column containing Chelex 100 resin (Bio-Rad), which had been previously washed and equilibrated with $^2H_2O$ at pH 7.4, to remove metal ions. The sample was then concentrated, and 150 mM NaCl (to approximate physiological ionic strength) and 5 mM Tris·HCl (both dissolved in $^2H_2O$) were added to achieve a final sample volume of 550 $\mu$L. This sample was used in a calcium titration monitored by two-dimensional NMR, performed according to previously described methods (*19*). NMR data acquisition parameters are given in Table 1. Calcium additions were made from stock solutions assayed by atomic absorption spectroscopy corresponding to concentrations of 182 $\mu$M, 455 $\mu$M, 1.36 mM, 5.0 mM, 15.9 mM, and 38.6 mM. The pH of the sample

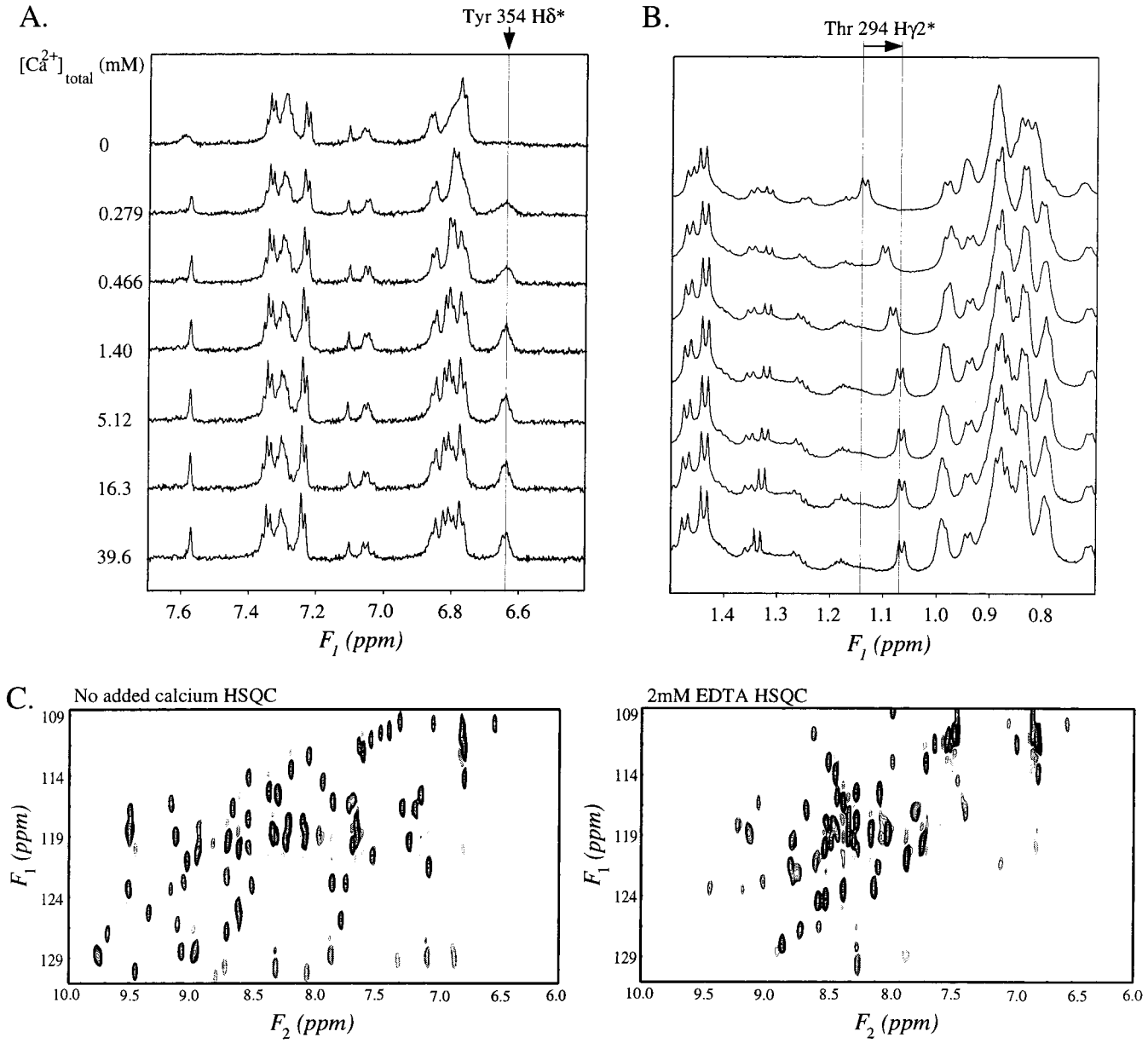


FIGURE 2: Selected regions of one-dimensional spectra of the LDLR EGF-AB pair acquired with increasing calcium concentration (A, B) and HSQC spectra acquired in the absence or presence of 2 mM EDTA, with no added calcium (C). In (A) the signal corresponding to the Hδ* protons of Tyr 354 becomes sharper but does not change position, suggesting saturation of the EGF-B site by a paramagnetic contaminant at the start of the titration. In (B) chemical shift perturbation of the Thr 294 methyl signal reveals the presence of a calcium binding site in EGF-A. The dramatic change in chemical shift dispersion observed in (C) upon metal ion removal from the B-site indicates a large conformational change associated with this transition.

was measured before and after each addition and maintained at 7.4 ± 0.1. The concentration of the NMR sample was measured by amino acid analysis at titration points 0, 2, 4, and 6 to be 291, 291, 261, and 233 $\mu$M, respectively. Standard regression analysis was used to curve fit the data using the equation

$$\Delta = \frac{\Delta_0 * [Ca^{2+}]_{free}}{K_d + [Ca^{2+}]_{free}} \quad (1)$$

to obtain a $K_d$ for the EGF-A site. In this equation $\Delta$ is the change in chemical shift at point *i*, $[Ca^{2+}]_{free}$ is the free calcium concentration at point *i*, and $\Delta_0$ is the total chemical shift change. The concentration of free $Ca^{2+}$ was calculated as described previously (*19*) using the equation

$$[Ca^{2+}]_{free} = [Ca^{2+}]_{tot} - (\Delta\Delta_0^{-1})[protein] \quad (2)$$

where $\Delta\Delta_0^{-1}$ is the fractional change in chemical shift.

*Fluorescence Measurement of $K_{d,av}$.* Measurement of changes in intrinsic protein fluorescence was also used to probe the calcium binding properties of the EGF-AB pair. While the sequence for the pair does not contain any Trp residues, there is a single Tyr in each domain, and changes in Tyr fluorescence have been used previously to characterize the calcium dissociation constant for a cbEGF domain from human fibrillin-1 (*34*). Two milliliter samples were prepared containing 4.8 (±0.2) $\mu$M EGF-AB (determined by amino acid analysis), 2 mM Tris·HCl, and 150 mM NaCl at pH 7.5. Blanks contained 2 mM Tris·HCl and 150 mM NaCl at pH 7.5. Lower concentration samples were assayed contain-

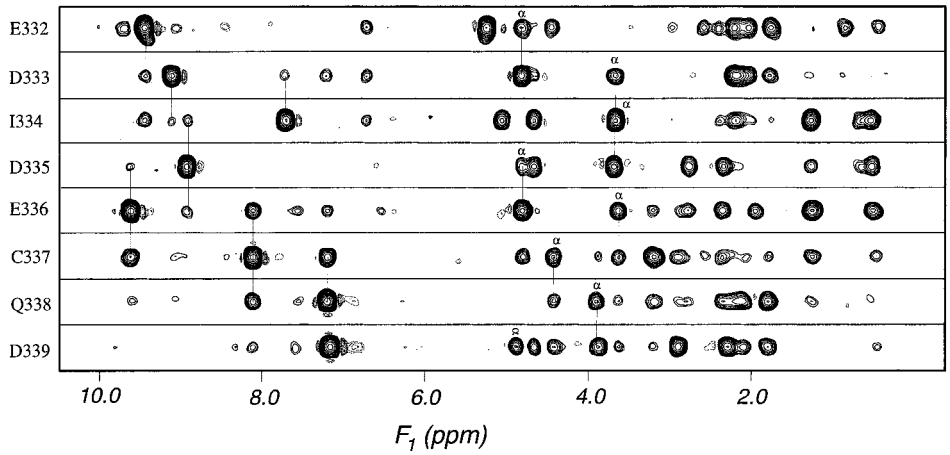


FIGURE 3: Selected region of sequentially assigned strips extracted from the three-dimensional $^{15}$N-edited NOESY-HSQC spectrum acquired at 30 °C and pH 6.5, $t_m$ = 150 ms. Sequential C$^\alpha$H−NH and NH−NH connectivities are joined by solid lines.

ing ~3 $\mu$M protein, but these did not yield adequate signal-to-noise ratios.

Emission spectra were recorded at 30 °C between 285 and 450 nm. The excitation wavelength was 277 nm, and the excitation and emission bandwidths were 5 and 10 nm, respectively. Fluorescence changes were observed at an emission wavelength corresponding to the maximum intensity measured in the absence of calcuim (308 nm). Initial titrations were performed using EDTA in order to estimate the concentration of metal ion contaminant, which was found to be 22 (±1) $\mu$M (data not shown). Therefore, 4.4 $\mu$L of a 10 mM EDTA stock was added to each sample to establish the 0 point. Qualitative comparison of the blank data indicated no significant fluorescence change associated with EDTA addition. In the first titration additions were made up to 10 mM $Ca^{2+}$, which demonstrated no change in fluorescence beyond a calcium concentration of 350 $\mu$M. Therefore, for the four final titrations, additions were made corresponding to total calcium concentrations of 5, 7.5, 10, 12.5, 15, 20, 25, 35, 55, 75, 95, 105, 170, 245, and 350 $\mu$M. Calcium stock solutions also contained 2 mM Tris·HCl and 150 mM NaCl at pH 7.5, and the volume of each addition was ≤4 $\mu$L. Standard regression analysis was used to curve fit the data using eq 1 to obtain an average dissociation constant for the two sites as described previously (*34*). $[Ca^{2+}]_{free}$ was calculated using eq 2, with $\Delta\Delta_0^{-1}$ equal to the fractional change in fluorescence intensity. In this analysis $\Delta$ is the change in fluorescence intensity at point *i*, $[Ca^{2+}]_{free}$ is the free calcium concentration at point *i*, $K_d$ is the average dissociation constant ($K_{d,av}$) for the two sites, and $\Delta_0$ is the total fluorescence change. Variable parameters in the fit were $K_d$ and $\Delta_0$.

*Chromophoric Chelator Measurement of Binding Constants*. Calcium binding properties of the EGF-AB pair were assayed using spectrophotometric analysis of competitive binding by 5,5′-$Br_2$-BAPTA (Molecular Probes) according to methods described by Linse et al. (*35*). These measurements were performed to confirm and refine dissociation constants measured by NMR and fluorescence methods. A calcium-free buffer solution was prepared containing 2 mM Tris·HCl and 150 mM NaCl, pH 7.5, and stored in a plastic container with dialysis tubing filled with Chelex 100 resin which had been previously equilibrated at pH 7.5. Purified protein (~3 mg) was dissolved in the calcium-free buffer, and the solution was incubated with Chelex 100 resin for 3 weeks to remove trace metal ion contaminants.

Absorbance scans and $Ca^{2+}$ titrations were performed using a dual-beam Lambda-20 UV−vis spectrophotometer (Perkin-Elmer, Norwalk, CT). Samples were prepared using the calcium-free buffer solution containing 25 $\mu$M 5,5′-$Br_2$-BAPTA and 15 (±2) $\mu$M protein with a total volume of 0.9 mL. The chelator concentration was determined on the basis of the extinction coefficient of the calcium-loaded form of 5,5′-$Br_2$-BAPTA ($\epsilon_{239.5}$ = 1.4 × $10^4$ $M^{-1}$) (*36*), and the protein concentration was measured by amino acid analysis. Blank samples were prepared equivalently without addition of protein, and measurements were referenced to a cell containing buffer alone. The residual calcium concentration of the samples was measured to be 4.8 $\mu$M on the basis of $A_{max}$ and $A_{min}$ measurements for samples containing saturating EDTA or $Ca^{2+}$, respectively.

Protein and blank samples were titrated sequentially using 1.5 or 2 $\mu$L additions of a 2.18 mM calcium stock (assayed by atomic absorption spectroscopy). After each addition the solution was mixed well and the absorbance at 263 nm read when a stable reading was obtained. This was repeated until no significant change occurred in $A_{263}$. A final addition of 2 $\mu$L of 1 M $CaCl_2$ was then made to complete saturation. The dissociation constant of the chelator was determined on the basis of the three blank titrations via least-squares fitting the data using the equation

$$A = (V_0/V_i)[A_{max} - (A_{max} - A_{min})]Y/(Y + K_{d,Q}) \quad (3)$$

in which $Y$ is the free calcium concentration at point *i*, $K_{d,Q}$ is the dissociation constant of the chelator−$Ca^{2+}$ complex, and $A_{max}$ and $A_{min}$ are the absorbances of $Ca^{2+}$-free and $Ca^{2+}$-saturated chelator in the absence of dilution, respectively. $V_0$ is the total volume at the start of the titration, and $V_i$ the total volume at titration point *i*, with dilution effects on the absorbance taken into account. $Y$ was taken as the positive root of the equation

$$Ca_{tot,i} = Y + [YC_{Q,i}/(Y + K_{d,Q})] \quad (4)$$

where the total calcium concentration at point *i* ($Ca_{tot,i}$) is expressed as a sum of free and bound $Ca^{2+}$ and $C_{Q,i}$ is the

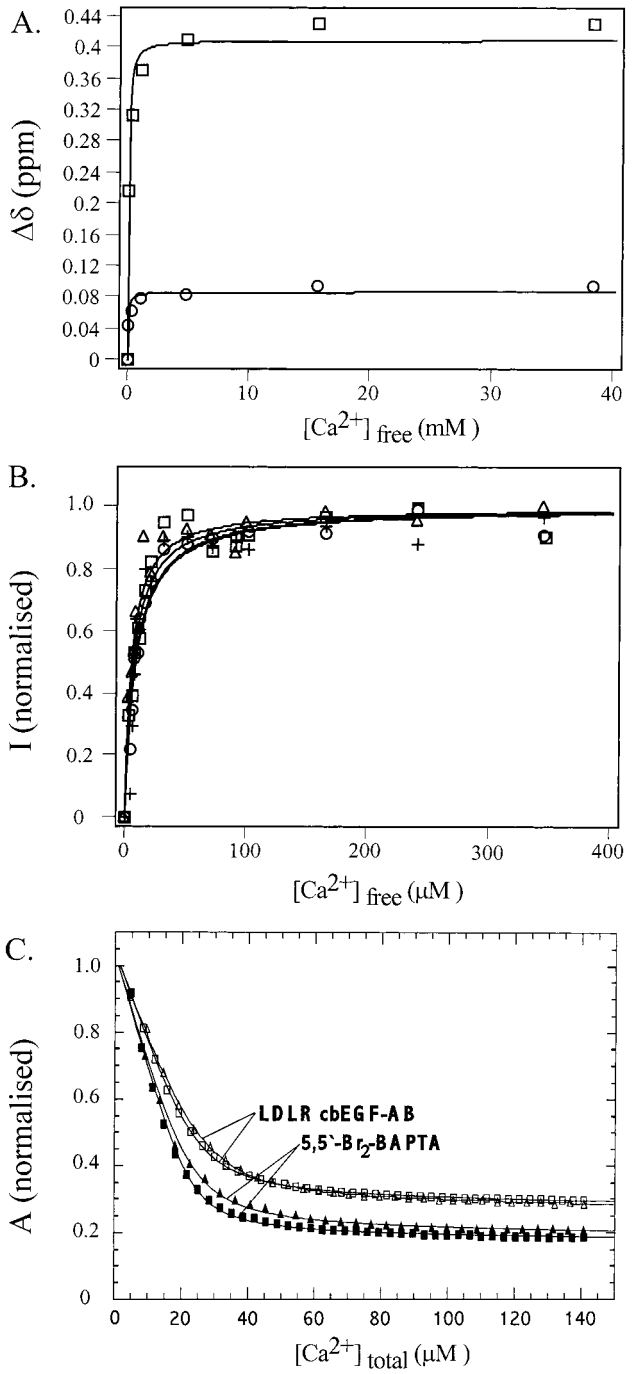


FIGURE 4: Curve fits to titration data acquired using (A) solution NMR, (B) intrinsic protein fluorescence, and (C) 5,5′-$Br_2$-BAPTA chromophoric chelator methods. In (A) the change in chemical shift as a function of free calcium is plotted for Thr 294 H$\gamma$2*−H$\beta$ (○), and the Tyr 315 H$\delta$*−H$\beta$2 (□) cross-peak is plotted. In (B) the normalized fluorescence intensity as a function of free calcium is plotted for each of the four titrations using different symbols (□, ○, △, +). In (C) a representative calcium titration of 5,5′-$Br_2$-BAPTA in the absence (■) and presence (□) of the LDLR cbEGF-AB pair is plotted for a titration performed using 1.5 $\mu$L additions.

chelator concentration at point *i*. Variable parameters in the fits were $K_{d,Q}$, $A_{max}$, and $A_{min}$.

Three titrations of EGF-AB were performed, although one data set was subsequently discarded due to anomalous results which may have been the result of pipeting errors or inadequate sample mixing or temperature calibration. Protein binding constants and the number of binding sites were then determined on the basis of least-squares fitting to the measured absorbance as a function of total calcium concentration using eq 3 as described previously (*35*, *37*). Variable parameters in the fits were the binding constants ($K_1$, $K_2$), $A_{max}$, and $A_{min}$. The number of sites (1 or 2) sensitive to the limit of detection of the assay was determined by evaluating the improvement in the ESS (error squared sum) as a function of adding the second site. An improvement of greater than 10-fold was considered significant (*38*).

## RESULTS

*NMR Characterization of the EGF-AB Pair*. Low-resolution mass spectrometry and assessment of one-dimensional spectra acquired in the presence and absence of added calcium suggested that the LDLR EGF-AB sample was homogeneous, monomeric, and folded in solution. Virtually complete $^1$H and $^{15}$N sequence-specific chemical shift assignments for the pair were made on the basis of a combination of two- and three-dimensional NMR spectra acquired on unlabeled and $^{15}$N-enriched samples. These assignments are given in Supporting Information, and representative strips from the three-dimensional $^{15}$N-edited NOESY-HSQC spectrum are shown in Figure 3. Assignment data were subsequently used in the analysis of the effects of calcium on one-dimensional spectra for the pair as shown in Figure 2. Surprisingly, while only the second EGF domain of the LDLR contains the consensus sequence associated with calcium binding (*11*−*13*), the data indicated the presence of an additional site in the EGF-A domain. In addition, comparison of spectra acquired with no added calcium versus in the presence of 2 mM EDTA suggested high affinity for the EGF-B site.

Two-dimensional homonuclear spectroscopy was utilized to characterize the binding properties of the pair according to previously described methods (*19*). Measurement of dissociation constants for cbEGF domains has typically relied on analysis of calcium-dependent chemical shift changes for $\delta$ ring protons of the conserved aromatic residue in the calcium binding consensus sequence (*19*, *34*, *39*−*42*) (see Figure 1B). On the basis of the chemical shift of the H$\delta$* protons for Tyr 354 in EGF-B, the attempt to remove calcium from the EGF-B site prior to the start of the titration was only partially successful. Some line broadening indicative of slow exchange between the calcium-loaded and calcium-free forms was observed, which is consistent with high-affinity binding at this site. Since NMR is best suited to measurement of dissociation constants ≥100 $\mu$M (*34*, *43*), only the dissociation constant for the noncanonical EGF-A site was characterized using this method.

It was not possible to use the calcium-dependent chemical shift changes of the H$\delta$* protons of the tyrosine in the EGF-A calcium binding site (Y315) for determination of the $K_d$ for this domain, due to near chemical shift degeneracy of the aromatic H$\delta$* and H$\epsilon$* protons in both the apo and holo forms. Therefore, two other cross-peaks with more significant chemical shift changes were assigned in the two-dimensional titration data and used in the analysis. These were Thr 294 H$\gamma$2*−H$\beta$ and Tyr 315 H$\delta$*−H$\beta$2; chemical shift changes for these peaks were analyzed in the $F_2$ and $F_1$ dimensions of the spectra, respectively. Curve fits to the change in chemical shift for each of these peaks as a function of free calcium concentration are shown in Figure 4A. Analysis of

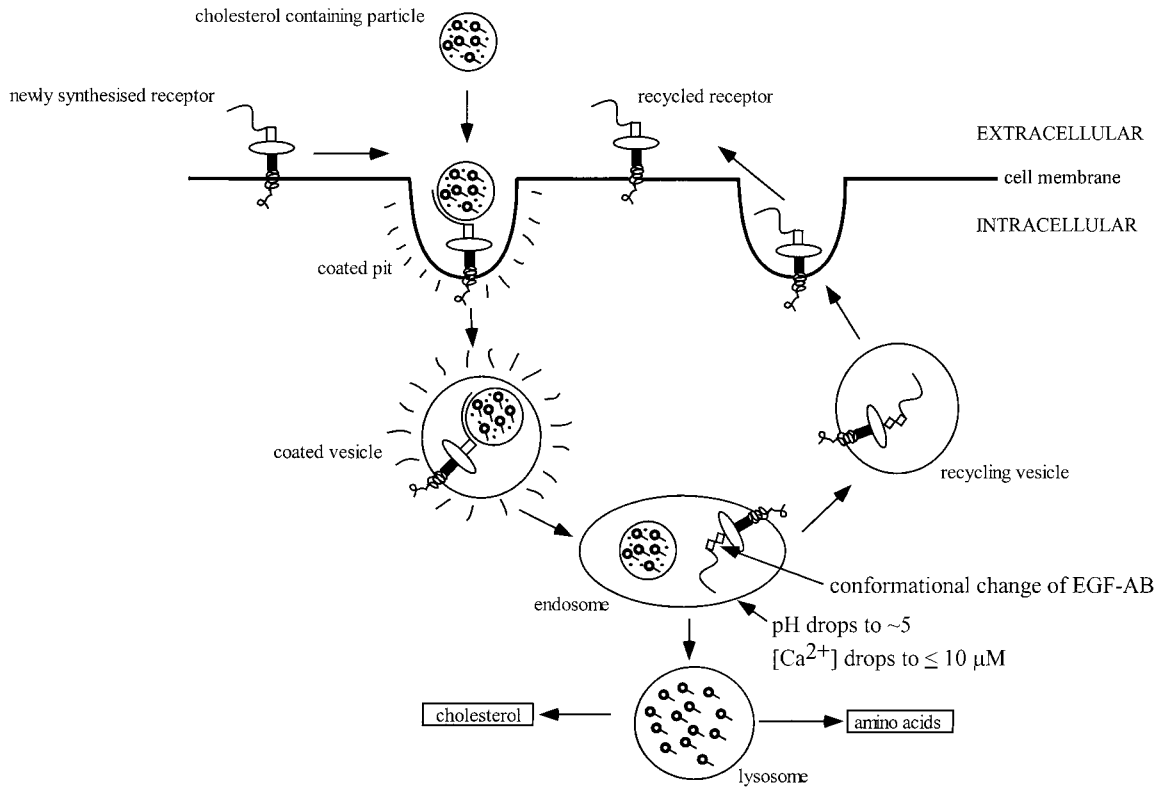


FIGURE 5: Schematic illustration of LDLR ligand binding and the receptor recycling pathway. Upon ligand binding, the LDLR−ligand complex is endocytosed. Under endosomal pH and calcium concentration conditions, the ligand is released. This process is proposed, on the basis of this study, to involve conformational change of the EGF-AB region of the receptor. The free receptor is then recycled to the cell surface to undergo another round of ligand binding.

the Thr 294 and Tyr 315 data yielded $K_d$ values of 46 (±16) $\mu$M and 41 (±11) $\mu$M, respectively, which are in good agreement.

*Characterization of EGF-AB Calcium Binding by Intrinsic Protein Fluorescence*. Measurement of changes in intrinsic protein fluorescence, which may be used to characterize higher affinity binding sites than NMR (*34*, *43*), was utilized to determine an average $K_d$ value for the EGF-A and EGF-B sites. Samples were initially titrated with EDTA until no further fluorescence change was observed to effectively remove divalent metal ions from the EGF-B site. Since the EGF-AB pair does not contain any Trp residues, changes in Tyr fluorescence were analyzed as a function of total calcium concentration. As shown in Figure 4B, the data for the four separate titrations are in good agreement, and analysis via curve fitting yielded an average $K_d$ of 7.2 (±1.6) $\mu$M. As noted above, this estimate for the $K_d$ represents an average for the two sites. However, qualitative comparison of the one- and two-dimensional NMR spectra acquired in the presence of 2 mM EDTA and at varying calcium concentrations suggests that this value is weighted toward the $K_d$ of the high affinity EGF-B site. This conclusion rests on the observation that while large conformational changes of the EGF-AB pair are associated with removal of calcium from the EGF-B site, only minor structural changes in the immediate vicinity of the EGF-A site are associated with the transition from the $Ca_1$ to $Ca_2$ form of the pair.

*Chromophoric Chelator Analysis of EGF-AB Calcium Binding Using 5,5′-Br$_2$-BAPTA*. Spectrophotometric analyses of changes in absorbance were utilized to evalute the dissociation constants of 5,5′-Br$_2$-BAPTA and EGF-AB. Analysis of the data for three titrations conducted on samples containing the chelator alone yielded a $K_d$ of 1.4 (±0.4) $\mu$M for 5,5′-Br$_2$-BAPTA in 150 mM NaCl and 2 mM Tris·HCl at pH 7.5, which agrees with the previously obtained value of 1.4 (±0.2) $\mu$M obtained under the same buffer conditions (*38*). This value was subsequently used in analysis of the titration data for samples containing both 5,5′-Br$_2$-BAPTA and EGF-AB. Best fits to the data, as illustrated in Figure 4C, were obtained when fitting only one of the calcium binding sites of the pair. The analysis yielded a $K_d$ value of 22 (±16) $\mu$M for the high-affinity site, which is in good agreement with the fluorescence results.

## DISCUSSION

Using a combination of biophysical methods, we have characterized two calcium binding sites in the EGF-AB pair of the low-density lipoprotein receptor. NMR, intrinsic protein fluorescence, and chemical chelator measurements are in good agreement and indicate that the dissociation constants for the sites are ~50 $\mu$M (A-site) and ~10−20 $\mu$M (B-site) at physiological ionic strength ($I$ = 0.15) and pH (7.4−7.5). Intriguingly, the EGF-A domain contains a noncanonical calcium binding sequence which binds with higher affinity than any N-terminal or isolated cbEGF domain that has been studied to date (*43*). A comparison of the domain sequences for the two EGF domains (Figure 1B) highlights that only the first ligand residue of the calcium binding consensus sequence is not conserved. On the basis of large NMR chemical shift changes of the Thr 294 H$\gamma$2* resonance upon calcium addition, it seems likely that this ligand is substituted by the Thr hydroxyl group in EGF-A. A search of the SWISS-PROT database (Release 39.6) (*44*) using a PROSITE pattern (*45*) revealed that this novel

calcium binding motif is conserved in LDL receptor sequences from other species, but it was not identified in any other proteins. This observation suggests that the EGF-A site may play a role in determining the specific biological properties of the LDL receptor with respect to other members of the LDLR gene family (*1*).

Qualitative analyses of changes in one- and two-dimensional NMR data indicate that while calcium binding to the higher affinity EGF-B site induces a large conformational adjustment of the pair, calcium occupancy of the A-site results in more localized structural changes. These observations are consistent with a recent report indicating that calcium plays a major role in defining the relative orientation of cbEGF domains in a pair from human fibrillin-1 (*46*).

The EGF precursor region of the LDL receptor is known to play a critical role in lipoprotein ligand dissociation from the receptor, a process that is strongly pH dependent. Since the effective calcium dissociation constant varies as a function of pH, the question arises whether the cbEGF domains undergo a calcium-dependent conformational change, which may be important in the ligand dissociation process (Figure 5). At present this hypothesis may only be evaluated in terms of calcium dissociation from the EGF-B site, since pairwise domain interactions can significantly affect the calcium binding properties of cbEGF domains (*34*, *42*). Recently, Rizzuto and co-workers measured the concentration of calcium in late vesicles using a calcium-sensitive photoreactive chimeric protein targeted to this cellular compartment as $\leq 10\ \mu$M (R. Rizzuto, University of Padova, personal communication). This result, taken together with this report, suggests that the $K_d$ of the EGF-B site is tuned to the calcium concentration in vesicles and that calcium plays an important role in the mechanism of the LDLR−ligand dissociation. Further experiments will be required to validate or disprove this hypothesis.

## ACKNOWLEDGMENT

The authors thank Penny Handford and Vroni Knott for assistance with LDLR EGF-AB sample preparation and useful discussions. Support for NMR experimentation by Jonathan Boyd, Nick Soffe, and Christina Redfield is also gratefully acknowledged.

## SUPPORTING INFORMATION AVAILABLE

A table of $^1$H and $^{15}$N chemical shifts for calcium-saturated LDLR EGF-AB, $T = 30$ °C, pH 6.5. This material is available free of charge via the Internet at http://pubs.acs.org.

## REFERENCES

1. Brown, M. S., Herz, J., and Goldstein, J. L. (1997) *Nature 388*, 629−630.
2. Goldstein, J. L., Brunschede, G. Y., and Brown, M. S. (1975) *J. Biol. Chem. 250*, 7854−7862.
3. Goldstein, J. L., Hobbs, H., and Brown, M. S. (1995) *The metabolic basis of inherited diseases*, 7th ed., McGraw-Hill, New York.
4. Hobbs, H. H., Brown, M. S., and Goldstein, J. L. (1992) *Hum. Mutat. 1*, 445−466.
5. Esser, V., Limbird, L. E., Brown, M. S., Goldstein, J. L., and Russell, D. W. (1988) *J. Biol. Chem. 263*, 13282−13290.
6. Russell, D. W., Brown, M. S., and Goldstein, J. L. (1989) *J. Biol. Chem. 264*, 21682−21688.
7. Sudhof, T. C., Goldstein, J. L., Brown, M. S., and Russell, D. W. (1985) *Science 228*, 815−822.
8. Yamamoto, T., Davis, C. G., Brown, M. S., Schneider, W. J., Casey, M. L., Goldstein, J. L., and Russell, D. W. (1984) *Cell 39*, 27−38.
9. Goldstein, J. L., and Brown, M. S. (1974) *J. Biol. Chem. 249*, 5153−5162.
10. Fass, D., Blacklow, S., Kim, P. S., and Berger, J. M. (1997) *Nature 388*, 691−693.
11. Handford, P. A., Mayhew, M., Baron, M., Winship, P. R., Campbell, I. D., and Brownlee, G. G. (1991) *Nature 351*, 164−167.
12. Mayhew, M., Handford, P., Baron, M., Tse, A. G. D., Campbell, I. D., and Brownlee, G. G. (1992) *Protein Eng. 5*, 489−494.
13. Rees, D. J. G., Jones, I. M., Handford, P. A., Walter, S. J., Esnouf, M. P., Smith, K. J., and Brownlee, G. G. (1988) *EMBO J. 7*, 2053−2061.
14. Blacklow, S. C., and Kim, P. S. (1996) *Nat. Struct. Biol. 3*, 758−762.
15. Varret, M., Rabes, J.-P., Thiart, R., Kotze, M. J., Baron, H., Cenarro, A., Descamps, O., Ebhardt, M., Hondelijn, J.-C., Kostner, G. M., Miyake, Y., Pocovi, M., Schmidt, H., Schmidt, H., Schuster, H., Stuhrmann, M., Yamamura, T., Junien, C., Beroud, C., and Boileau, C. (1998) *Nucleic Acids Res. 26*, 248−252.
16. van der Westhuyzen, D. R., Stein, M. L., Henderson, H. E., Marais, A. D., Fourie, A. M., and Coetzee, G. A. (1991) *Biochem. J. 278*, 677−682.
17. Davis, C. G., Goldstein, J. L., Südhof, T. C., Anderson, R. G. W., Russell, D. W., and Brown, M. S. (1987) *Nature 326*, 760−765.
18. Raleigh, E. A., Murray, N. E., Revel, H., Blumenthal, R. M., Westaway, D., Reith, A. D., Rigby, P. W. J., Elhai, J., and Hanahan, D. (1988) *Nucleic Acids Res. 16*, 1563−1575.
19. Knott, V., Downing, A. K., Cardy, C. M., and Handford, P. (1996) *J. Mol. Biol. 255*, 22−27.
20. Jeener, J., Meier, B. H., Bachmann, P., and Ernst, R. R. (1979) *J. Chem. Phys. 71*, 4546−4553.
21. Macura, S., Huang, Y., Suter, D., and Ernst, R. R. (1981) *J. Magn. Reson. 43*, 259−281.
22. Aue, W. P., Bartholdi, E., and Ernst, R. R. (1976) *J. Chem. Phys. 64*, 2229−2246.
23. Brown, S. C., Weber, P. L., and Mueller, L. (1988) *J. Magn. Reson. 77*, 166−169.
24. Braunschweiler, L. R., and Ernst, R. R. (1983) *J. Magn. Reson. 53*, 521−528.
25. Bax, A., and Davis, D. G. (1985) *J. Magn. Reson. 65*, 355−360.
26. Bodenhausen, G., and Ruben, D. J. (1980) *Chem. Phys. Lett. 69*, 185−189.
27. Kay, L. E., Keifer, P., and Saarinen, T. (1992) *J. Am. Chem. Soc. 114*, 10663−10665.
28. Kay, L. E., Marion, D., and Bax, A. (1989) *J. Magn. Reson. 84*, 72−84.
29. John, B. K., Plant, D., Webb, P., and Hurd, R. E. (1992) *J. Magn. Reson. 98*, 200−206.
30. Zhu, G., and Bax, A. (1990) *J. Magn. Reson. 90*, 405−410.
31. Wuthrich, K. (1986) *NMR of Proteins and Nucleic Acids*, John Wiley, New York.
32. Cavanagh, J., Fairbrother, W. J., Palmer, A. G., III, and Skelton, N. J. (1996) *Protein NMR Spectroscopy*, Academic Press Inc., San Diego, CA.
33. Johnson, B. A., and Blevins, R. A. (1994) *J. Biomol. NMR 4*, 603−614.
34. Smallridge, R. S., Whiteman, P., Doering, K., Handford, P. A., and Downing, A. K. (1999) *J. Mol. Biol. 286*, 661−668.
35. Linse, S., Johansson, C., Brodin, P., Grundström, T., Drakenberg, T., and Forsén, S. (1991) *Biochemistry 30*, 154−162.
36. Haugland, R. (1996) *Handbook of fluorescent probes and research chemicals*, Molecular Probes, Inc., Eugene, OR.
37. Dahlback, B., Hildebrand, B., and Linse, S. (1990) *J. Biol. Chem. 265*, 18481−18489.

38. Rand, M. D., Lindblom, A., Carlson, J., Villoutreix, B. O., and Stenflo, J. (1997) *Protein Sci. 6*, 2059−2071.
39. Handford, P. A., Baron, M., Mayhew, M., Willis, A., Beesley, T., Brownlee, G. G., and Campbell, I. D. (1990) *EMBO J. 9*, 475−480.
40. Handford, P. A., Downing, A. K., Rao, Z., Hewett, D. R., Sykes, B. C., and Kielty, C. M. (1995) *J. Biol. Chem. 270*, 6751−6756.
41. Whiteman, P., Downing, A. K., Smallridge, R., Winship, P. R., and Handford, P. A. (1998) *J. Biol. Chem. 273*, 7807−7813.
42. Kettle, S., Yuan, X., Grundy, G., Knott, V., Downing, A. K., and Handford, P. A. (1999) *J. Mol. Biol. 285*, 1277−1287.
43. Downing, A. K., Handford, P. A., and Campbell, I. D. (2000) *Top. Biol. Inorg. Chem. 3*, 83−99.
44. Bairoch, A., and Apweiler, R. (1999) *Nucleic Acids Res. 27*, 49−54.
45. Hofmann, K., Bucher, P., Falquet, L., and Bairoch, A. (1999) *Nucleic Acids Res. 27*, 215−219.
46. Werner, J. M., Knott, V., Handford, P. A., Campbell, I. D., and Downing, A. K. (2000) *J. Mol. Biol. 296*, 1065−1078.

BI002322L